DESIGN AND EXPERIMENTAL STUDY ON TWIN-SCREW STRAW PULPING MACHINE
/
稻秆双螺杆制浆机设计与试验

Huiting CHENG, Nan ZHAO, Dezhi REN, Wei WANG, Yuanjuan GONG, Wanyuan HUANG [1]
College of Engineering, Shenyang Agricultural University, Shenyang/ China
Tel: +86-15909822656; E-mail: 2022500013@syau.edu.cn
Corresponding author: Huang Wanyuan
DOI: https://doi.org/10.35633/inmateh-75-15

Keywords: *rice straw; finite element analysis; Ab-T_{10} breakage model; twin-screw; biomechanical pulping*

ABSTRACT

Despite the abundance of agricultural straw as a renewable resource, its low utilization efficiency remains a significant challenge due to inadequate mechanical processing methods. To solve the problem, the ANSYS finite element simulation software was employed to simulate and analyze two screw configurations (parallel and staggered arrangement) and four compression zone designs. The optimal coupling breaking method was determined to be the parallel type with a 2-2-2 compression zone combination for the twin-screw system. Based on the simulation results, a twin-screw straw pulping machine was constructed. The test factors included screw speed, thread pitch, and straw moisture content, with straw breaking rate as the test index. Simulation test was conducted to optimize the structural parameters of the twin-screw straw pulping machine, followed by a verification test. The results indicated that at a screw speed of 120 r/min, a thread pitch of 203 mm, and a straw moisture content of 60%, the straw breaking rate was the highest at 79.9%. The verification test results were consistent with the simulation results, with less than 5% deviation, confirming the reliability of the simulation model and optimization outcomes. This paper provides a basis for the design and optimization of twin-screw pulping machines and offers theoretical support for the high-value utilization of agricultural waste through enhanced mechanical processing technologies.

摘要

尽管农业秸秆作为一种可再生资源非常丰富，但由于机械加工方法不足，其利用效率低下仍然是一个重大挑战。为了解决这个问题，采用 ANSYS 有限元仿真软件，对并列型与错列型 2 种螺杆配置和 4 种压缩区设计进行模拟分析，确定最佳耦合碾压破碎方式为并列型 2-2-2 压缩区组合的双螺杆，根据仿真结果试制稻秆双螺杆制浆机。以螺杆转速、螺纹间距和稻秆含水率为试验因素，以稻秆破碎率为试验指标，通过仿真试验对稻秆双螺杆制浆机进行结构参数优化，并进行验证试验。试验表明：螺杆转速为 120r/min，螺纹间距为 203mm，秸秆含水率为 60%时，秸秆破碎率最高为 79.9%；验证试验结果与仿真结果具有一致性，误差小于 5%，仿真模型和优化结果具有可靠性。本文为双螺杆制浆机的设计和优化提供了依据，为通过强化机械加工技术实现农业废弃物的高值化利用提供了理论支持。

INTRODUCTION

China has an abundant production of straw, and the raw materialization of straw is an important direction for its high-value utilization. However, the utilization rate of raw materialization is only 2.1%, which is one of the main factors constraining the improvement of the comprehensive utilization rate of straw (*Hirani et al., 2018*). Currently, straw pulping is one of the emerging methods for straw raw material utilization *(Subramaniyan et al., 2022)*. The annual production of rice straw exceeds 200 million tons, accounting for about 22.74% of the total agricultural straw production, and the production is only less than that of corn straw (*Gong et al., 2019*). Therefore, the study of rice straw pulping is of great significance for improving the comprehensive utilization rate of straw, promoting sustainable agricultural development, alleviating the current shortage of pulp, and reducing the dependence on foreign trade in pulp.

Cheng Huiting, Ph.D. Stud. Eng.; Zhao Nan, MS. Stud. Eng.; REN Dezhi, Lec. Ph.D. Eng.; Wang Wei, Prof. Ph.D. Eng.; Gong Yuanjuan, Prof. Ph.D. Eng.; Huang Wanyuan, Lec. Ph.D. Eng.

Chemical pulping, mechanical pulping, and two-stage pulping are the principal pulping methods currently (*Li et al., 2023*). The traditional chemical pulping method is technologically mature but poses significant environmental challenges.

The mechanical pulping method is mainly applicable to wood pulping, when used in agricultural straw and other non-wood raw materials pulping, the obtained pulp often exhibits inferior quality and cannot meet industry standards. The two-stage pulping method combines chemical or biological pre-treatment with mechanical refining post-treatment in the pulping process. Pulp obtained from non-wood raw materials using this method is of better quality than that produced by mechanical pulping, making the two-stage pulping method suitable for pulping agricultural straw and other non-wood raw materials. The two-stage pulping method is mainly divided into chemical mechanical pulping (CMP) and biological mechanical pulping (BMP). The BMP method is more environmentally friendly in terms of reduced chemical usage and lower wastewater generation.

With the emergence of BMP technology, scholars have conducted extensive research on the biological pre-treatment processes of non-wood raw materials such as rice straw (*Guan et al., 2018*), corn straw (*Qing et al., 2017*), and wheat straw (*Kang et al., 2021*). However, significant challenges remain in the preparation stage of non-wood bio-mechanical pulp, highlighting the need for specialized equipment development to advance BMP technology. Twin-screw pulping machines have emerged as the primary choice for pulping equipment due to their high breaking efficiency and fibrillating capacity (*Arthur and Rahmanian, 2024*), yet research in this area in China is still in its infancy. *Kowalski et al.* used MDT software to design and analyze co-rotating twin-screw extruders for food applications (*Kowalski et al., 2018*); Düphans applied CAD/CAE technology for the design and simulation of twin-screw pulping machinery (*Düphans et al., 2024*). These studies are limited to the design of twin-screw components and have not yet addressed the complete machine design and optimization of twin-screw pulping machines. Fleur utilized Ludovic simulation software to optimize the twin-screw pulping machine, improving the production efficiency of cellulose nanofibrils and reducing energy consumption through the simulation and optimization of screw profiles (*Rol et al. 2020*). The physical and chemical properties and the matched twin-screw pulping machine are different from the BMP method for the pretreatment of wooden raw materials and the pulping raw materials produced by the chemical method. Therefore, it is of great significance to design and optimize a twin-screw pulping machine with BMP pulping technology for rice straw as raw material to promote the comprehensive utilization of straw. Rol optimized the twin-screw extrusion process through simulation software, achieving efficient production of high-quality cellulose nanofibrils (CNF), demonstrating the feasibility of simulation design in the field of pulping machinery design and optimization (*Rol et al., 2019*).

In this paper, ANSYS finite element simulation software is used to determine the flow channel structure and the combination of compression zones of the twin-screw device, designing and constructing a twin-screw pulping machine. Based on the previously calibrated Ab-T10 breaking model, the Rocky discrete element simulation software is employed to simulate the breaking process of straw particles. Through a three-factor quadratic orthogonal rotational combination simulation test, the effects of screw speed, thread pitch, and straw moisture content on the breaking rate of rice straw were investigated to optimize the working and structural parameters of the twin-screw pulping machine, thereby increasing the breaking rate of rice straw. The accuracy and reliability of the model are verified by comparing the results of the simulation with those of the validation tests.

MATERIALS AND METHODS

Twin screw pulping machine design

Structure and Working Principle

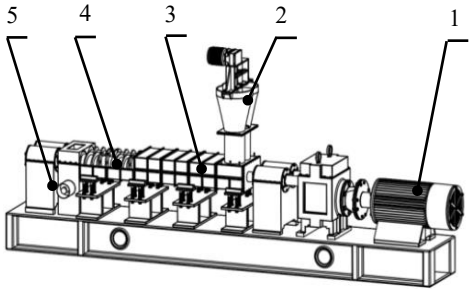

Fig. 1 - Three-dimensional model of the twin-screw pulping machine of rice straw

1 - Motor; 2 - Material feeding device; 3 - Grinding device; 4 - Grinding twin screw; 5 - Discharging device

The structure of the twin-screw pulping machine is shown in Figure 1, which mainly consists of a grinding device, an electric motor, a material feeding device, and a discharge device. During operation, rice straw is placed into the feed opening of the material feeding device at a uniform speed and in appropriate amounts to avoid blockages. The straw first enters the pulping machine through the feeding device, and after being crushed, sheared, and broken by the twin-screw grinding device, it is sent to the discharge device, where the broken pulp is collected.

Selection and design of threaded elements

The cross-section of screw elements is typically rectangular or serrated. The asymmetry of serrated screw elements enhances the mixing of materials, promotes the dispersion of fibers, and refines the pulp, thereby improving the pulping quality. Compared to the traditional rectangular cross-section, serrated screw elements are more suitable for the compression and homogenization stages of the pulping process. The shearing action can effectively improve the flowability of the material, reduce retention phenomena, and enhance uniformity and efficiency. Therefore, screw elements with a serrated cross-section were used, as shown in Figure 2.

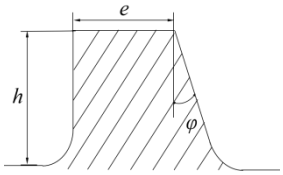

Fig. 2 - Thread cross-section shape

The screw diameter directly affects the material processing capacity and the power consumption of the device, while the screw length is related to the residence time of the material within the screw, which in turn affects the pulping efficiency (*Lyashuk et al., 2022*). Screw elements are commonly selected in sizes of 180 mm, 240 mm, 300 mm, 350 mm, etc. Based on the laboratory equipment conditions, screw elements with an outer diameter of 180mm were chosen. The optimal diameter range of 60-200 mm ensures efficient material conveying, mixing and processing capabilities while maintaining compatibility with existing equipment *(Delvar et al., 2025)*.

$$h = (0.02 \sim 0.2)D_e \quad (1)$$

$$e = (0.08 \sim 0.12)D_e \quad (2)$$

where: h is the groove depth, mm; e is the width of normal screw prong, mm; D_e is the outer diameter of the screw, mm.

Design of thread pitch

The pitch of the screw thread affects the fill rate of the material in the screw and its flow characteristics. A smaller pitch can increase the fill rate of the material, but may lead to hindered material flow and increased screw wear, affecting the shearing action of the screw on the material. A larger pitch can provide stronger shearing forces, which is beneficial for material mixing and the disruption of the cellulose structure, but it also increases the wear on the screw. According to the transport rate of solid materials and the theory of pulp flow, the thread lift angle φ should be designed between 17° and 30° to ensure effective transport and mixing of the material within the screw. Based on equations (3) and (4), the range of pitch values can be calculated to be 172~326 mm.

$$S = \pi \cdot D_e \tan\varphi \quad (3)$$

where: S is the lead, mm; φ is the thread rising angle, °.

$$S = pz \quad (4)$$

where: p is the thread pitch, mm; z is the number of threads, z=1.

Design of structural clearance

During pulping, the pulping raw materials exhibit the characteristics of soft solids, hence the clearances can be selected to be on the larger side.

$$\delta_a = (0.01 \sim 0.03)D_e \quad (5)$$

According to equation (5), the range of values for the gap σ_a between the top of the screw prong and the shaft were calculated as 1.8~5.4 mm. The smaller the σ_a, the less the leakage flow and the higher the conveying efficiency, but the mixing effect is reduced. Therefore, σ_a was chosen to be 3 mm.

At this clearance value, the equipment can maintain a certain conveying efficiency while keeping pressure fluctuations and friction between the screw and barrel moderate, thus avoiding excessive energy consumption.

$$\delta_b = (0.01 \sim 0.02) D_e \tag{6}$$

According to equation (6), the range of the gap between the twin screws δ_b was calculated as 1.8~3.6 mm. The smaller the δ_b, the higher the manufacturing precision required for the twin screws. Therefore, δ_b was chosen to be 3 mm. With this clearance, material flows stably between the twin screws, allowing sufficient time for mixing and shearing without over-pressurization or excessive residence time, which could cause overheating or degradation, thus enhancing pulp quality consistency.

$$C_L = D_e + \delta_b \tag{7}$$

Therefore, according to equation (7), the center distance C_L between the twin screws was calculated to be 180.3 mm, which ensures a moderate gap between the screws, avoiding material residue and ensuring efficient shearing and mixing effects.

$$D_s = D_e + 2\delta_a \tag{8}$$

From equation (8), the internal diameter D_S of the shaft was calculated to be 180.6 mm.

TWIN-SCREW COUPLING SIMULATION DESIGN

By integrating numerical computation and finite element simulation methods (*Zhang et al. 2023*), the two established flow channel models were simulated under various conditions by ANSYS 2022 R1. By comparing the pressure field distribution of the two flow channels, the coupling method for the twin-screw straw pulping machine was selected. Using the finite element simulation method and the selected twin-screw coupling method, the four established compression zone models were simulated under various conditions. By comparing the flow of material between the screws, the compression zone combination method for the twin-screw straw pulping machine was selected.

Model Establishment

(1) Flow Channel Model Establishment

The screws of twin-screw pulping machines are often designed in a modular fashion, allowing the installation of thread elements on the core shaft as needed, with single-start threads commonly used (*Gu et al., 2019*). The coupling forms between thread elements are divided into parallel and staggered types, as shown in Figure 3(a). Based on the uniform continuous mixing and transportation mechanism (*Düphans et al., 2024*), the parallel thread element coupling model used single-start thread screws; based on the shear dispersion uniformization mechanism (*Kolomiets and Jirout, 2021*), the staggered thread element coupling model used a 180° staggered configuration of single-start thread elements. With the Boolean operation modeling capabilities of SolidWorks software, the flow channel structure models corresponding to the two types of twin-screw coupling models were constructed, as shown in Figure 3(b).

a. Twin-screw coupling model *b. Structural modeling of channels* *c. Twin-screw coupling model* *d. Structural modeling of channels*

Fig. 3 - The model of twin-screw and flow channel

(2) Compression Zone Model Establishment

Positive threads have the function of conveying and compressing material, while reverse threads have the function of blocking material and increasing pressure. When the material was pushed from the positive thread to the reverse thread to the next thread area, the material was compressed and sheared under the extrusion of the positive and reverse threads. The flow channel area formed by the positive and reverse threads is a compression zone. A twin-screw device generally have three compression zones, and each segment of thread elements forming the compression zone should have 2-3 threads.

The compression zones are combined with two types, positive threaded element-reverse threaded element (referred to as 1) and reverse threaded element-positive threaded element (referred to as 2). Using SolidWorks software, four types of compression zone combination models were established as shown in Figure 4.

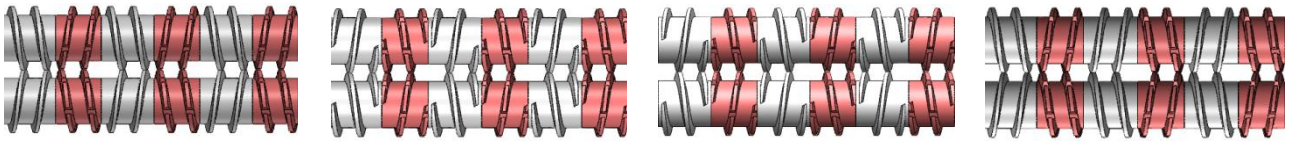

a. 1-1-1 *b. 2-2-2* *c. 1-2-2* *d. 2-1-1*

Fig. 4 - Compression zone combination model

Meshing and Simulation Parameter Settings

The model was imported into Ansys software (*Xiao et al. 2024*), and hexahedral meshing was used to optimize computational efficiency and accuracy. Local mesh refinement was performed on complex areas of the screws and flow channels to analyze the flow characteristics of the material within the channels. The rheological model of the straw pulp was set to the power-law fluid model to describe its non-Newtonian characteristics (*Liu et al. 2019*). The material properties of the rice straw pulp were shown in Table 1, Twin-screw material parameters were shown in Table 2.

Table 1

Physical parameters of straw pulp

Parameter	Value	Parameter	Value
Straw pulp consistency	682	density	232.3 kg/m^3
Power law index	0.49	specific heat capacity	6.585 J/(kg·K)
Temperature coefficient	0.042 K^{-1}	heat transfer coefficient	0.2 W/(m·K)
Reference temperature	373.15 K		

Table 2

Twin-screw material parameters

Part	Material	Density/kg·m^{-3}	Elastic modulus/MPa	Poisson's ratio
Shaft core	42CrMo	7850	2.06×10^5	0.28
Threaded element	A_2 tool steel	7860	2.06×10^5	0.28

The twin-screw rotation speed was set to 120 r/min, the entrance velocity of the rice straw pulp was set to 1 m/s, and a pressure outlet boundary condition was used. The inner wall was set to a no-slip boundary condition, using the no-slip option in Ansys-Fluent to ensure no relative sliding between the pulp and the device walls. The initial temperature was set to 25^o C, the initial pressure was set to 101325 Pa, the time step was set to 0.01 seconds, the number of iterations was set to 500, and the relaxation factor was set to 0.7 to accelerate convergence. The Euler multiphase flow model was used to simulate the motion of the mixed phase of the straw pulp, capturing the flow characteristics of the straw pulp in the twin-screw device.

Dynamic Solution of Straw Pulp

To accurately analyze the dynamic characteristics of straw pulp within the crushing flow channel, the following assumptions were made: the effects of gravity and inertia forces in the flow field were neglected; the straw pulp was assumed to move in a laminar flow within the crushing device, completely filling the device and behaving as an incompressible fluid; the straw pulp was assumed to move without slippage within the cavity of the crushing device. Based on the constitutive equations of fluid dynamics and the rheological properties of the fluid, numerical simulation and analysis of the flow of straw pulp under isothermal and non-isothermal conditions were performed.

To describe the changes in the volumetric flow rate of straw pulp and the dynamic relationship between fluid density and velocity field, the conservation of straw pulp phase material during the crushing process was captured according to the continuity equation, as shown in equation (9). This equation demonstrates the conservation of mass of the straw pulp and its flow behavior within the channel during the crushing process by considering the vector velocity and density.

$$\nabla \bullet (\rho \vec{v}) + \frac{\partial \rho}{\partial t} = 0 \tag{9}$$

where: $\vec{v}$ is the vector velocity of straw pulp, m/s; ρ is the straw pulp density, kg/m^3.

The internal momentum transfer mechanism of straw pulp during the crushing process was described by the Navier-Stokes equation, as shown in equation (10). The equation reveals the mechanism of internal momentum transfer and transformation within the straw pulp during the crushing phase and enables the prediction of the flow patterns of the pulp based on relevant parameters.

$$\rho(\frac{\partial \vec{v}}{\partial t}+(\vec{v}\bullet\nabla)\vec{v})=-\nabla p+\nabla\bullet\vec{\tau}+\vec{f}_v \tag{10}$$

where: p is the static pressure on straw pulp, Pa; $\vec{\tau}$ is the stress tensor of straw pulp, Pa; $\vec{f}_v$ is the Volumetric force of straw pulp, N/m^3.

Energy conservation equation expresses the thermodynamic behavior of straw pulp through changes in internal energy, heat exchange with the environment, and energy loss due to fluid flow, as shown in equation (11). This equation quantifies the change in internal energy of the straw pulp during crushing, taking into account the energy alterations caused by molecular thermal motion and interactions, thereby analyzing the energy trajectory of the straw pulp throughout the crushing process.

$$\rho C_p(\frac{\partial T}{\partial t}+\vec{v}\bullet\nabla T)=\nabla\bullet(k\nabla T)+\frac{\vec{\tau}}{\nabla\vec{v}} \tag{11}$$

where: C_p is the specific heat capacity, J/(kg·K); T is the temperature, K. ∇T is the temperature gradient, K/m; $\nabla\vec{v}$ is the velocity gradient tensor, s^{-1}; k is the heat transfer coefficient, W/(m·K).

Straw pulp conform to the characteristics of pseudoplastic fluids *(Terashima et al., 2022)*. Under isothermal conditions, power-law model is used to describe rheological behavior as shown in equation (12). This equation illustrates the variation in the flow characteristics of straw pulp under different shear rates in an isothermal environment.

$$\eta=m\dot{\gamma}^{(n-1)} \tag{12}$$

where: η is the straw pulp viscosity, Pa·s; m is the straw pulp consistency, Pa·s^n; n is the power law index of straw pulp; $\dot{\gamma}$ is the shear rate tensor of straw pulp, s^{-1}.

Under non-isothermal conditions, the rheological behavior of straw pulp is significantly affected by temperature, and is represented by a temperature-dependent rheological model *(Gienau et al., 2018)*. Equation (13) describes the relationship between the apparent viscosity (η) of straw pulp and the shear rate (γ) as well as temperature. The function $H(T)$ is temperature-dependent, serving to adjust the viscosity to reflect the effects of temperature variations.

$$\eta=m\dot{\gamma}^{(n-1)}\cdot H(T) \tag{13}$$

$$H(T)=\exp[-\beta(T-T_\alpha)] \tag{14}$$

where: T is the temperature, K; β is the temperature coefficient of straw pulp, K^{-1}; T_α is the reference temperature for straw pulp, K.

SIMULATION ANALYSIS AND OPTIMIZATION OF RICE STRAW PARTICLE BREAKING

Test factors and indicators

Rice straw pre-treated by biological method was selected as the test material. In accordance with the requirements of the "HJ/T 340-2007 Clean Production Standard for the Papermaking Industry" standard, pretreated rice straw was made into oven dried pulp with a moisture content of 10%, followed by the testing samples with different moisture contents prepared using biofungal liquid and drying method.

To optimize the working performance of the rice straw twin-screw pulping machine, based on preliminary design and pretesting, the thread pitch, screw speed, and rice straw moisture content were taken as the test factors. Based on the previous section on design, the range of thread pitch was 172~326 mm; the range of screw speed was 100~140 r/min (*Jiang et al., 2024*); considering the characteristics of rice straw material, the moisture content range for rice straw was taken as 50~70% (*Cheng et al., 2022*). Based on the function of the rice straw twin-screw pulping machine, the rice straw breaking rate was chosen as the evaluation index of its working performance, and the calculation formula is as follows:

$$P=\frac{m_b}{m_t}\times 100\% \tag{15}$$

where: m_b is the mass of broken particles, g; β is the total mass of particle sample, g.

Test Design

The discrete element model of rice straw particles established by Jiang and others, along with the parameter calibration results of the Ab-T10 crushing model (*Jiang et al., 2024*), and the mechanical model constructed in this paper were imported into the Rocky DEM 4.5 to simulate the crushing process of rice straw particles and conduct a three-factor quadratic orthogonal central composite simulation test, and the factor level coding table is shown in the table 3. The screen aperture diameter x_1, pitch x_2, and blade and shell clearance x_3 are the actual values of the factors.

Table 3

Coding table

Code	Screw speed (x_1)/r/min	Thread pitch (x_2)/mm	Moisture content (x_3)/%
-1.682	100	172	50
-1	108	203	54
0	120	249	60
+1	132	295	66
+1.682	140	326	70

RESULTS

Simulation results and analysis

Simulation results and analysis of twin-screw channel characteristics

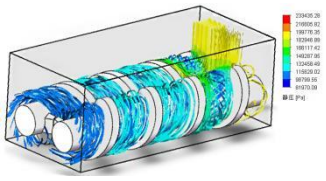

a. parallel type *b. staggered type*

Fig. 5 - Flow channel pressure field

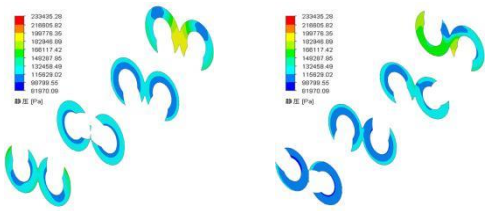

a. parallel type *b. staggered type*

Fig. 6 - Cross-section of pressure field

Figure 5(a) showed a mirror symmetry in the pressure gradients of the left and right flow channels, with the maximum pressure difference being less than 0.5 MPa. This symmetry was particularly evident in the screw engagement area, where symmetrical High-Pressure Ridges formed, and peak pressures were concentrated at the thread top clearance. The symmetric pressure field suppressed the lateral exchange of materials through the force equilibrium, indicating a lateral flow velocity of less than 0.1 m/s, which aligned with the flow characteristics dominated by laminar flow, where the Reynolds Number is approximately 120 *(Saldana et al., 2024)*. The symmetric high-pressure area created a uniform shear stress field of about 450 kPa, which continuously acted on the straw particles through viscous dissipation, promoting the uniform delamination of cellulose microfibrils.

Figure 5(b) showed a significantly higher pressure peak in the left flow channel compared to the right. Local pressure discontinuities greater than 3 MPa/mm occurred at the thread top clearance and engagement area, leading to a substantial lateral pressure difference. This asymmetry triggered secondary flows, increasing the lateral flow velocity to 0.6 m/s and inducing vortices, with the flow state exhibiting transitional turbulence characteristics, where the Reynolds Number is about 450. The high pressure difference drove fibers to undergo bending-shear coupled damage in the engagement area. However, the local peak shear stress exceeded the yield strength of the straw fibers, and the uneven stress distribution resulted in a mixture of over-pulverized particles and unbroken coarse grains.

Figure 6(a) showed a cross-sectional pressure distribution that decreased in a concentric circular pattern, aligning with the predicted trend of the Generalized Herschel-Bulkley Model. Near the wall, the shear rate was synchronized with the compression-relaxation cycle of the thread clearance, forming periodic stress loading that facilitated the progressive disintegration of fibers.

Figure 6(b) showed a cross-sectional pressure field with a left-high and right-low gradient, generating a normal pressure component that compelled fibers to migrate along an inclined path, increasing the likelihood of collisions with the flight flanks. A low-pressure vortex area appeared at the bottom of the right flow channel, increasing the average residence time for some fibers and intensifying the risk of thermal degradation.

The simulation results showed that the pressure distribution of the left and right channels of the parallel type is almost symmetric in the twin-screw, keeping the material transfer and pressure state in the channel uniform. Such symmetric pressure distribution reduced the cross exchange of straw particles in the engaging area, which made the material flow more stable and continuous.

It is more favorable to destroy the structure of cellulose, hence the parallel type has more uniform effect on the grinding and shearing action of the material. The pressure distribution in the left and right flow channels with staggered thread element coupling exhibited asymmetry, especially at the screw crests and in the meshing zone. The asymmetric pressure distribution created a transverse pressure difference across the grooves, causing the shearing force experienced by straw fibers in the meshing zone to be uneven, leading to an uneven crushing and breaking effect on the straw particles.

Consequently, to ensure the pulping effect and quality of the twin-screw pulping machine, the twin-screw with parallel thread element was selected as the core breaking element of the breaking device in the twin-screw pulping machine.

Compression zone simulation results and analysis

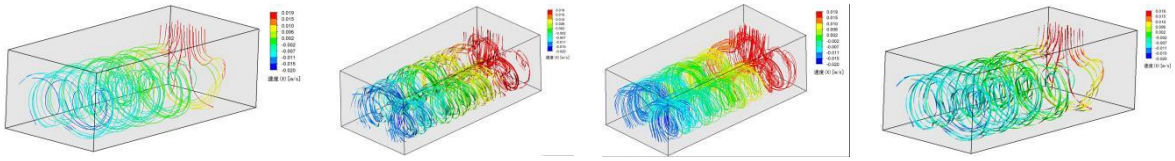

a. 1-1-1 *b. 2-2-2* *c. 1-2-2* *d. 2-1-1*

Fig. 7 - Compression zone combination velocity field

The simulation results of the four compression zones were shown in Figure 7. From Figure (a), the flow field of the 1-1-1 configuration exhibited a low-gradient uniform distribution. No significant velocity shear layer was formed between the twin screws, leading to a lower shear rate. The analysis of the flow lines indicated that the material primarily moved axially in the engagement area, with a low rate of lateral migration. Due to insufficient shear strength, the straw fibers underwent only limited disintegration, resulting in a higher retention of fiber length and a lower proportion of hydrogen bonds being broken, which caused uneven dispersion of the fiber bundles.

From Figure (b), it was observed that in the engagement area of the 2-2-2 twin screw configuration, symmetrical "V" shaped high-speed shear zones were formed. Within this region, uniform velocity gradients led to the generation of uniform shear layers, with the flow field symmetry index reaching as high as 0.92. The velocity components of the material in the axial and radial directions approached a ratio of 1:1, promoting three-dimensional mixing. The preliminary shearing action in the "V" shaped area, in conjunction with the reverse shearing action in the inverted "V" shaped area, created a cyclic loading mechanism. This mechanism significantly enhanced the efficiency of hydrogen bond breaking, effectively increased the fiber surface area, and resulted in a concentrated particle size distribution, achieving efficient crushing and dispersion. Additionally, this velocity field had good stability, which could effectively reduce the material residence time, making it the optimal configuration.

From Figure (c), the 1-2-2 configuration exhibited an asymmetric velocity distribution, with the peak velocity in the left flow channel being higher than that in the right, creating an inclined shear zone. The generation of localized vortices enhanced mixing, but the distribution of shear rates was uneven. The reverse shearing in the inverted "V" region led to a coupling of fiber bending and tearing, which reduced the proportion of coarse fibers but resulted in over-pulverization.

From Figure (d), the 2-1-1 configuration resulted in velocity dead zones between the screws, with the primary shear area being confined near the thread clearance. The streamlines indicated that the material circulated and lingered within these dead zones, leading to localized temperature increases and thermal degradation. The efficiency of fiber disintegration was relatively low, and the particle size distribution exhibited a bimodal pattern, indicating a coexistence of insufficient fragmentation and over-pulverization.

As shown in Figure 7, the 2-2-2 and 1-2-2 compression zone combinations created strong shear zones, enhancing the shearing and mixing of straw particles between the twin screws and improving their breaking efficiency. Under the action of the twin screws, straw particles entered the "V" shaped area and underwent pre-shearing, where fibers begin to separate. After entering the inverted "V" shaped area, straw particles were subjected to reverse shear forces, further breaking the hydrogen bonds between fibers, increasing the surface area of the fibers, and promoting the effective dispersion of fiber bundles. The 2-2-2 configuration demonstrated superior symmetry in the velocity distribution field compared to the 1-2-2 combination, ensuring more uniform transport of rice straw material through the flow channel and reducing flow instability caused by uneven pressure distribution.

The movement of rice straw in the 2-2-2 flow channel was more stable, and the shearing action was more uniform, which is conducive to the destruction of the cellulose structure and the dispersion of fiber bundles. Therefore, the twin-screw with the in-line 2-2-2 compression zone combination was used as the core breaking element of the breaking device in the twin-screw pulping machine.

Simulation Results and Analysis of the Crushing Process

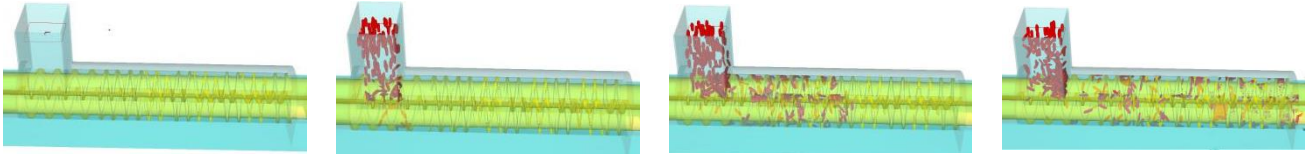

a. *0s* *b. 5s* *c. 10s* *d. 15s*

Fig. 8 - Simulation of straw particles crushing process in pulping machine

The Rocky simulation software was utilized to simulate and analyze the breaking process of straw particles from the feeding side to the crushing side, as shown in Figure 8.

Test results and analysis

The simulation results of the breaking process for rice straw particles are shown in Table 4, where *A*, *B*, and *C* were the factor encoding values. The experimental data were analyzed using Analysis of Variance (ANOVA) to determine the significance of the factors affecting the rice straw breaking rate. The ANOVA was conducted using the Design-Expert software, which provided a comprehensive analysis of the variance components and their corresponding F-values and P-values. The regression equation for the rice straw breaking rate (*P*c) was derived from the ANOVA results, and the significance of each term in the equation was assessed. The optimization of the process parameters was performed using the Response Surface Methodology (RSM) in Design-Expert software, which allowed for the determination of the optimal screw speed, thread spacing, and straw moisture content to maximize the breaking rate. The results of the ANOVA was presented in Table 5.

Table 4

Test design and results

No.	Screw speed (*A*)/r/min	Thread Pitch (*B*)/mm	Moisture content (*C*)/%	Breaking rate (*Pc*)/%
1	1	1	1	48
2	1	1	-1	54.5
3	1	-1	1	54.25
4	1	-1	-1	56.75
5	-1	1	1	52.3
6	-1	1	-1	55.6
7	-1	-1	1	62.75
8	-1	-1	-1	51.25
9	1.682	0	0	52.75
10	-1.682	0	0	61
11	0	1.682	0	64.5
12	0	-1.682	0	51.75
13	0	0	1.682	51.25
14	0	0	-1.682	70.75
15	0	0	0	68.25
16	0	0	0	72.25
17	0	0	0	70.75
18	0	0	0	70.5
19	0	0	0	70
20	0	0	0	70.5
21	0	0	0	75
22	0	0	0	70.75
23	0	0	0	74

Table 5

Analysis of variance

Source	SS	Freedom	MS	*F*-value	*P*-value
Model	1492.76	9	165.86	7.03	0.0010
A	36.33	1	36.33	1.54	0.0064
B	3.43	1	3.43	0.1455	0.0090
C	82.65	1	82.65	3.51	0.0038
AB	0.7200	1	0.7200	0.0305	0.0040
AC	36.98	1	36.98	1.57	0.0325
BC	44.18	1	44.18	1.87	0.1942
A^2	540.49	1	540.49	22.92	0.0004
B^2	461.69	1	461.69	19.58	0.0007
C^2	303.99	1	303.99	12.89	0.0033
Residual	66.54	13	6.58		
Lack of fit	71.79	5	9.36	12.51	0.1013
Error	34.75	8	4.34		
Total value	1799.30	22			0.0010

From Table 5, it is known that the regression equation model has a *P*-value less than 0.01, indicating a highly significant result. The lack of fit item has a *P*-value of 0.1013, which suggests a good fit of the equation. The thread pitch, screw speed, rice straw moisture content, interaction terms *AB*, and the quadratic terms A^2,

B^2, C^2 have a highly significant effect on the rice straw crushing rate (P<0.01). The interaction terms AC and BC have a significant effect on the rice straw breaking rate (P<0.05). Under the interaction effects, the order of influence of each factor on the rice straw breaking rate is moisture content > thread pitch > screw speed. After eliminating the non-significant terms, the regression model for the encoded values of the rice straw breaking rate (Pc) is:

$$P_C = 71.41 - 1.63A + 0.5012B - 2.46C - 0.3000AB - 2.15AC - 2.35BC - 5.83A^2 - 5.39B^2 - 4.37C^2 \quad (16)$$

The optimal working parameters were obtained using the Optimization Numerical module of Design-Expert 8.0.6 software and based on Equation 16. When the screw speed was 120 r/min, the thread pitch was 203 mm, and the rice straw moisture content was 60%, the rice straw breaking rate reached its highest value of 79.9%.

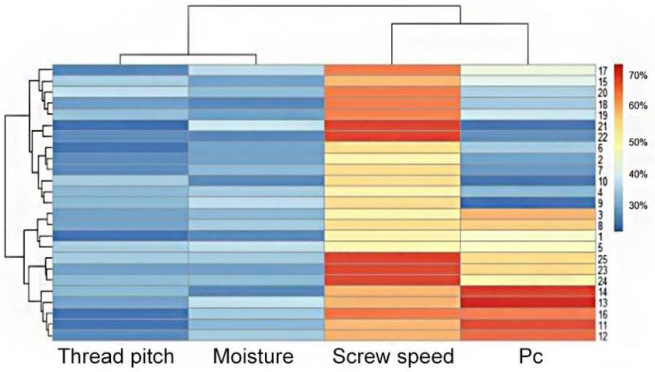

Fig. 9 - The influence of screw speed, thread pitch and straw moisture content on straw pulp rate

As shown in Figure 9, the screw speed has a significant impact on the rice straw breaking rate. When the screw speed is less than 120 r/min, the rice straw breaking rate tends to increase, and it begins to decrease after exceeding 120 r/min. This phenomenon can be attributed to the enhancement of mixing and shearing of the material by the screw as the speed increases (*Fan et al., 2023*). When the speed exceeds 120 r/min, the residence time of the material in the screw is shortened, reducing the breaking of the material, leading to a decrease in the breaking rate. The effect of rice straw moisture content on the rice straw breaking rate is relatively smaller. The rice straw breaking rate increases with the increase of moisture content until it reaches 60% and then begins to decrease. The expansion degree of the rice straw material increases with the increase of moisture content, leading to an increase in hardness and viscosity, a decrease in the filling density of the material in the screw, and a reduction in contact and shearing between the materials, which reduces the breaking effect. The effect of screw thread pitch on the rice straw crushing rate is the least significant. When the thread pitch is less than 203 mm, the rice straw breaking rate tends to increase, which is attributed to the increased contact frequency between the rice straw and the screw, thereby enhancing the shearing and breaking effects. When the thread pitch reaches 203 mm, the rice straw breaking rate decreases, which may be due to the overly wide pitch reducing the effective contact and shearing of the material. The effective contact and shearing of rice straw between the screws are reduced, lowering the local pressure and shearing force.

Test bench test verification

a. Rice straw twin-screw pulping machine *b. Rice straw particle grinding and breaking process*

Fig. 10 - Verification test of rice straw particle breakage

Rice straw was prepared into test samples with a moisture content of 60% according to the methods previously described. Based on the simulation optimization results, the twin-screw rotation speed was set to 120 r/min, and the thread pitch was set to 203 mm. Under the optimal parameter combination, a validation test on the breaking of rice straw particles was conducted using the rice straw twin-screw pulping machine, as shown in Figure 10. To reduce random error, five replicate tests were performed.

The test values of the rice straw breaking rate were 82.7%, 78.6%, 83.4%, 81.3%, and 84.1%, with an average of 82.02% and an error value of 2.6%. The error between the simulation test results and the actual test results was less than 5%, indicating that the results of the simulation optimization are accurate. Furthermore, the proposed model demonstrates significant potential for broader applicability across diverse straw material systems (e.g., wheat, corn, and barley straws), while also providing a method to explore the intricate chemical reactions during pulping, thereby revealing the pulping mechanism.

CONCLUSIONS

(1) The ANSYS analysis software was used to conduct simulation analysis on two flow channel structures and four compression zone combinations. ANSYS analysis software was used to simulate two flow channel structures and four compression zone combinations. Results showed that the parallel 2-2-2 compression zone combination in the twin-screw design offered significant advantages in mixing and extruding rice straw material, providing a more uniform force environment compared to the staggered coupling, which performed poorly in the same speed range. This finding provides a practical basis for optimizing pulping equipment design, enabling the selection of efficient structural configurations for industrial-scale straw processing, thereby enhancing production efficiency and reducing energy consumption.

(2) Based on the simulation analysis results and the characteristics of rice straw material, a rice straw twin-screw pulping machine was designed with a screw outer diameter of 180 mm, a thread pitch range of 172~326 mm, a clearance of 3 mm between the top of the screw thread and the shaft, a clearance of 3 mm between the twin-screws, and a barrel inner diameter of 180.6 mm. This design enables industrial-scale rice straw pulping, supporting sustainable development in straw-based industries.

(3) The calibrated Ab-T_{10} breaking model and Rocky simulation software were used to perform a three-factor quadratic orthogonal central composite simulation experiment, and a validation test was conducted using the rice straw twin-screw pulping machine. The simulation results showed that the order of influence on the straw breaking rate was: moisture content > thread pitch > screw speed. When the screw speed was 120 r/min, the thread pitch was 203 mm, and the straw moisture content was 60%, the maximum rice straw breaking rate was 79.9%. The validation test results indicated that the error between the simulation and actual test results was 2.6%, and the simulation results basically matched the actual situation, confirming the reliability of the optimization results for the rice straw twin-screw pulping machine. These findings provide a practical foundation for the design and optimization of industrial-scale pulping equipment, promoting the high-value utilization of agricultural waste.

ACKNOWLEDGEMENT

This research was funded by the Project supported by the National Natural Science Foundation of China（32171900）.

REFERENCES

[1] Arthur T.B., & Rahmanian N., (2024). Process Simulation of Twin-Screw Granulation: A Review. *Pharmaceutics*, Vol.16, no.6, pp.706, Switzerland. DOI:10.3390/pharmaceutics16060706

[2] Cheng H.T., Gong Y.J., Zhao N., Zhang L.J., Lv D.Q., Ren D.Z., (2022). Simulation and Experimental Validation on the Effect of Twin-Screw Pulping Technology Upon Straw Pulping Performance Based on Tavares Mathematical Model. *Processes*, Vol.10, no.11, pp.2336, Switzerland. DOI:10.3390/pr10112336

[3] Delvar E., Oliveira I., Brito M.S.C.A., Silva C.G., Santamaria-Echart A., Barreiro M.F., Santos R.J., (2025). Literature Review on Single and Twin-Screw Extruders Design for Polymerization Using CFD Simulation. *Fluids*, Vol.10, no.1, pp.9, Switzerland. DOI:10.3390/fluids10010009

[4] Düphans V., Kimmel V., Messing L., Schaldach G., Thommes M., (2024). Experimental and Numerical Characterization of Screw Elements Used in Twin-Screw Extrusion. *Pharmaceutical Development and Technology*, Vol.29, no.7, pp.675-683, England. DOI:10.1080/10837450.2024.2378323

[5] Fan Z.P., Ma Z., Wang H.B., Yu Z.H., (2023). Optimization of Screw Conveying of Kneaded Corn Stalks Based on Discrete Element Method. *INMATEH Agricultural Engineering*, Vol.69, no.1, pp.626-634, Romania. DOI:10.35633/inmateh-69-60

[6] Gienau T., Kraume M., Rosenberger S., (2018). Rheological Characterization of Anaerobic Sludge from Agricultural and Bio-Waste Biogas Plants. *Chemie Ingenieur Technik*, Vol.90, no.7, pp.988-997, Germany. DOI:10.1002/cite.201700102

[7] Gong Y.J., Deng N., Bai X.W., Huang W.Y., Liu D.J., (2019). Detection of Corn Straw Components by Fourier Transform Infrared Spectroscopy (玉米秸秆组分的傅里叶红外光谱检测). *Taiyangneng Xuebao/Acta Energiae Solaris Sinica*, Vol.40, no.6, pp.1664-1671, China. DOI:10.19912/j.0254-0096.2019.06.024.

[8] Gu B.J., Dhumal G.S., Wolcott M.P., Ganjyal G.M., (2019). Disruption of Lignocellulosic Biomass Along the Length of the Screws with Different Screw Elements in a Twin-Screw Extruder. *Bioresource Technology*, Vol.275, pp.266-271, England. DOI: 10.1016/j.biortech.2018.12.033

[9] Guan R.L., Li X.J., Wachemo A.C., Yuan H.R., Liu Y.P., Zou D.X., Zuo X.Y., Gu J.Y., (2018). Enhancing Anaerobic Digestion Performance and Degradation of Lignocellulosic Components of Rice Straw by Combined Biological and Chemical Pretreatment. *Science of The Total Environment*, Vol.637-638, pp.9-17, Netherlands. DOI:10.1016/j.scitotenv.2018.04.366

[10] Hirani A.H., Javed N., Asif M., Basu S.K., Kumar A., (2018). A Review on First- and Second-Generation Biofuel Productions. *Biofuels: Greenhouse Gas Mitigation and Global Warming: Next Generation Biofuels and Role of Biotechnology,* pp.141–154, India. DOI:10.1007/978-81-322-3763-1_8

[11] Jiang S.Y., Ren D.Z., Ma F., Chen Z.Y., Che Y.M., (2024). Parameter Calibration of Rice Straw Particle–Crushing Model. *Engenharia Agrícola*, Vol.44, pp.e20240063, Spain.

[12] Kang Y.R., Su Y., Wang J., Chu Y.X., Tian G., He R., (2021). Effects of Different Pretreatment Methods on Biogas Production and Microbial Community in Anaerobic Digestion of Wheat Straw. *Environmental Science and Pollution Research*, Vol.28, no.37, pp.51772-51785, DOI: 10.1007/s11356-021-14296-5

[13] Kolomiets A., Jirout T., (2021). Analysis of the Dispersion of Viscoelastic Clusters in the Industrial Rotor-Stator Equipment. *Processes*, Vol.9, no.12, pp.2232, Switzerland. DOI: 10.3390/pr9122232

[14] Kowalski R.J., Hause J.P., Joyner H., Ganjyal G.M., (2018). Waxy Flour Degradation – Impact of Screw Geometry and Specific Mechanical Energy in a Co-Rotating Twin Screw Extruder. *Food Chemistry*, Vol.239, pp.688-696, England. DOI: 10.1016/j.foodchem.2017.06.120

[15] Li P.W., Xu Y.P., Yin L., Liang X.L., Wang R.M., Liu K.Q., (2023). Development of Raw Materials and Technology for Pulping—a Brief Review. *Polymers*, Vol.15, NO.22, pp.44-65, Switzerland. DOI:10.3390/polym15224465

[16] Liu Y.Q., Chen J.J., Song J., Hai Z., Lu X.H., Ji X.Y., Wang C.S., (2019). Adjusting the Rheological Properties of Corn-Straw Slurry to Reduce the Agitation Power Consumption in Anaerobic Digestion. *Bioresource Technology*, Vol.272, pp.360-369, England. DOI: 10.1016/j.biortech.2018.10.050

[17] Lyashuk O.L., Hevko I.B., Hud V.Z., Tkachenko I.G., Hevko O.V., Sokol M.O., Tson O.P., Kobelnyk V.R., Shmatko D.Z., Stanko A.I., (2022). Research of Non-Resonant Oscillations of the Telescopic Screw - Fluid Medium System. *INMATEH Agricultural Engineering*, Vol.68, no.3, pp.499-510, Romania. DOI:10.35633/inmateh-68-49

[18] Qing Q., Zhou L.L., Guo Q., Gao X.H., Zhang Y., He Y.C., Zhang Y., (2017). Mild Alkaline Presoaking and Organosolv Pretreatment of Corn Stover and Their Impacts on Corn Stover Composition, Structure, and Digestibility. *Bioresource Technology*, Vol.233, pp.284-290, England.

[19] Rol F., Vergnes B., El Kissi N., Bras J., (2020). Nanocellulose Production by Twin-Screw Extrusion: Simulation of the Screw Profile to Increase the Productivity. *ACS Sustainable Chemistry & Engineering*, Vol.8, no.1, pp.50-59, Washington. DOI: 10.1021/acssuschemeng.9b01913

[20] Saldana M., Gallegos S., Gálvez E., Castillo J., Salinas-Rodríguez E., Cerecedo-Sáenz E., Hernández-Ávila J., Navarra A., Toro N., (2024). The Reynolds Number: A Journey from Its Origin to Modern Applications. *Fluids*, Vol.9, no.12, pp.299, Switzerland. DOI: 10.3390/fluids9120299

[21] Subramaniyan S.K., Rajkumar J., Santhanam S.S., Raja K., Lakshmanan G., (2022). Preliminary Studies on the Production of Paper from Millet Husk and Rice Straw. *Environmental Engineering and Management Journal*, Vol.21, no.9, pp.1545-1555, Romania. DOI: 10.30638/eemj.2022.137

[22] Terashima M., Kotegawa Y., Sun M., Liu B., Yasui H., (2022). Modeling Thixotropic Break-Down Behavior of Dense Anaerobically Digested Sludge. *Applied Rheology*, Vol.32, no.1, pp.1-7, Poland. DOI:10.1515/arh-2022-0121

[23] Xiao W.S., Niu P., Wang P., Xie Y.j., Xia F., (2024). Simulation Analysis and Optimization of Soil Cutting of Rotary Blade by Ansys/Ls-Dyna. *INMATEH Agricultural Engineering*, Vol.72, no.1, pp.22-32, Romania. DOI:10.35633/inmateh-72-02

[24] Zhang F.K., Shao W.X., Zhao S.J., Zhu J.K., Li P., (2023). Simulation Test and Verification of Material Conveying for Small and Medium-Sized Air Suction Jujube Picking Machine Based on CFD-DEM Coupling. *INMATEH Agricultural Engineering*, Vol.71(3),.535-547, DOI: 10.35633/inmateh-71-46